British Journal of Pharmacology (2005) 146, 397–407
www.nature.com/bjp

Ion transport regulated by protease-activated receptor 2 in human airway Calu-3 epithelia

[1]Shinji Sato, *,[1]Yasushi Ito, [1]Masashi Kondo, [1]Takamasa Ohashi, [1]Satoru Ito, [2]Shinsuke Nakayama, [1]Kaoru Shimokata & [1]Hiroaki Kume

[1]Department of Respiratory Medicine, Nagoya University Graduate School of Medicine, 65 Tsurumai-cho, Showa-ku, Nagoya, Aichi 466-8550, Japan and [2]Department of Cell Physiology, Nagoya University Graduate School of Medicine, 65 Tsurumai-cho, Showa-ku, Nagoya, 466-8550, Japan

1 We examined the mechanisms underlying anion secretion mediated by protease-activated receptor 2 (PAR2) and its role in the regulation of ion transport, using polarized human airway Calu-3 cells.

2 PAR2 stimulation by trypsin and a PAR2-activating peptide (PAR2AP), especially from the basolateral aspect, caused transient Cl^- secretion due to cytosolic Ca^{2+} mobilization.

3 Antagonists of PI-PLC (U73122, ET-18-OCH_3) and inositol 1,4,5-triphosphate (xestospongin C (Xest C)) were without effect on the PAR2AP-mediated Cl^- secretion, whereas it was attenuated by D609 (a PC-PLC inhibitor) and phorbol 12-myristate 13 acetate (PMA, a PKC activator).

4 Even 30 min after removal of PAR2AP after a 10-min-exposure, cells were still poorly responsive to PAR2 stimulation, but the reduced responsiveness was upregulated by a PKC inhibitor, GF109203X (GFX).

5 Pretreatment with PAR2AP did not affect responses to anion secretagogues, such as isoproterenol, forskolin, thapsigargin, 1-ethyl-2-benzimdazolinone, and adenosine, but ATP-induced responses were significantly reduced. Nystatin permeabilization studies revealed that the presence of PAR2AP prevented ATP-induced increments in basolateral membrane K^+ conductance without affecting apical membrane Cl^- conductance.

6 ATP-elicited Ca^{2+} mobilization, which was sensitive to D609 and PMA, was inhibited by the pretreatment with PAR2AP, and this inhibition was blunted by the presence of GFX.

7 Collectively, stimulation of PAR2 generates a brief response of Cl^- secretion through PC-PLC-mediated pathway, followed by not only auto-desensitization of PAR2 itself but also cross-desensitization of a PC-PLC-coupled purinoceptor. The two types of desensitization seem likely to have PKC-mediated downregulation of PC-PLC in common.
British Journal of Pharmacology (2005) **146,** 397–407. doi:10.1038/sj.bjp.0706330;
published online 11 July 2005

Keywords: Protease-activated receptor 2; airway ion transport; desensitization; Cl^- secretion; phosphatidylcholine-phospholipase C; purinoceptor; protein kinase C

Abbreviations: $[Ca^{2+}]_i$, cytosolic Ca^{2+} concentration; CFTR, cystic fibrosis transmembrane conductance regulator; DAG, diacylglycerol; 1-EBIO, 1-ethyl-2-benzimdazolinone; GFX, GF109203X; G_t, transepithelial conductance; hIK-1 channel, human intermediate conductance, inward-rectifying Ca^{2+}-activated K^+ channel; I_{Cl}, apical membrane Cl^- current; I_{eq}, equivalent short-circuit current; I_K, basolateral membrane K^+ current; Ins P_3, inositol 1,4,5-triphosphate; NHBE, normal human bronchial epithelial cells; PAR2, protease-activated receptor 2; PAR2AP, PAR2-activating peptide; PC-PLC, phosphatidylcholine-phospholipase C; PD, transepithelial potential difference; PI-PLC, phosphatidylinositol-phospholipase C; PKC, protein kinase C; PSS, physiological saline solution; $P2Y_1R$, $P2Y_1$ purinoceptor; revPAR2AP, the reverse sequence peptide of PAR2-activating peptide; Xest C, xestospongin C

Introduction

Protease-activated receptors (PARs) belong to a family of seven transmembrane G protein-coupled receptors that are activated by extracellular proteases (Macfarlane *et al*., 2001). These receptors are activated by the proteolytic unmasking of a receptor-bound, NH_2-terminal-tethered ligand domain, which is then able to interact with the extracellular loop of the receptor itself and initiate signaling. To date, four PARs (PAR1–4) have been characterized (Macfarlane *et al*., 2001). Thrombin activates PAR1, -3, and -4, whereas trypsin and mast cell tryptase activate PAR2 and possibly PAR4 (Macfarlane *et al*., 2001). Synthetic peptides based on the receptor-activating sequence of the tethered ligand can directly bind and activate the receptors (Dery *et al*., 1998). Various branches of science have been paying growing attention to the functional relevance of PARs, because of their systemic distribution and potential roles in numerous systems, including homeostasis, inflammation, and the regulation of smooth muscle tone (Dery *et al*., 1998; Cocks *et al*., 1999; Cocks & Moffatt, 2001; Macfarlane *et al*., 2001). PAR2 is the PAR predominantly expressed in human airway epithelia (Cocks & Moffatt, 2000). Recently, upregulation of PAR2 in the

*Author for correspondence; E-mail: itoyasu@med.nagoya-u.ac.jp

respiratory epithelium of patients with bronchial asthma was reported (Knight *et al*., 2001). Further, Northern blotting analysis of human tissues shows that trypsin-like protease mRNA is most prominently expressed in tracheal tissue, suggesting that this protease is localized in the airway (Yamaoka *et al*., 1998). These reports implicate PAR2 in the pathophysiology of chronic obstructive airway diseases.

It is well known that the chronic obstructive airway diseases share aspects of mucous congestive diseases (Kellerman, 2002), in which excessive and tenacious mucus secretion causes airway obstruction and is involved in the morbidity and mortality of these diseases (Lundgren & Shelhamer, 1990; Aikawa *et al*., 1992). In particular, bronchial gland cells predominantly contribute to airway electrolyte secretion, which is accompanied by fluid movement, thereby forming low viscosity mucus to maintain efficient mucociliary clearance (Shimura, 2000). Despite the significance of the electrolyte transport system in airway conductivity, little is known regarding the roles of PAR2 in this system. Thus, the aim of the present study was to establish how Cl^- secretion is regulated by PAR2-mediated signals, using polarized Calu-3 epithelia, which is a model of human airway submucosal gland serous cells (Devor *et al*., 1999). Through the investigations, we also found that PAR2 stimulation caused not only auto-desensitization but also cross-desensitization of a purinoceptor that is well known as a key molecule promoting mucociliary clearance in the airway (Ramminger *et al*., 1999; Inglis *et al*., 2000; Ito *et al*., 2004a).

Methods

Cell culture

Calu-3 human airway cells (American Type Culture Collection, Manassas, VA, U.S.A.) at passages 29–35 were grown in a 1 : 1 mixture of Dulbecco's Modified Eagle's Medium and Ham's F-12 (Invitrogen, Carlsbad, CA, U.S.A.) containing 10% fetal bovine serum (Invitrogen), 100 μg/ml streptomycin, and 100 U/ml penicillin (Invitrogen). The cells were maintained in tissue-culture flasks (T75) at 37°C in a 95% air–5% CO_2 humidified incubator. After reaching 80–90% confluence, cells were detached using a solution of PBS, 0.04% EDTA, and 0.25% trypsin. The collected cells were passaged with a 1 : 4 dilution of the same solution and seeded onto porous polyester membranes (0.4 μm pore size on Snapwell or Transwell inserts, 1.1 cm^2, Costar, Cambridge, MA, U.S.A.) at a density of 10^6 cells/well. The inserts had been collagen-coated overnight with 0.2% human placental collagen type VI (Sigma-Aldrich, St Louis, MO, U.S.A.). The day after seeding the cells on the filters, the medium remaining on the apical side was removed to establish an air interface, which markedly improves the differentiation of human airway epithelia in a well-polarized fashion (Shen *et al*., 1994). The cells were fed by replacement of the basolateral medium every 48 h. Experiments were carried out after 7–13 days in culture.

Normal human bronchial epithelial cells (NHBE; BioWhittaker, Walkersville, MD, U.S.A.) seeded into T75 flasks were grown for detection of PAR2 mRNA in bronchial epithelial cell growth medium (BEGM; BioWhittaker) supplemented with bovine pituitary extract (52 μg ml^{-1}), hydrocortisone (0.5 μg ml^{-1}), human recombinant epidermal growth factor (0.5 ng ml^{-1}), epinephrine (0.5 μg ml^{-1}), transferrin (10 μg ml^{-1}), insulin (5 μg ml^{-1}), retinoic acid (0.1 μg ml^{-1}), triiodothyronine (6.5 μg ml^{-1}), gentamycin (50 μg ml^{-1}), and amphotericin B (50 μg ml^{-1}). The medium was changed every 48 h until cells were 90% confluent.

RT–PCR for detection of PAR2 mRNA

Total RNA was extracted from Calu-3 and NHBE cells, which had been grown to near confluence on T75 flasks, using Trizol reagent (Invitrogen). First-strand cDNA was generated using SuperScript III (Invitrogen) and random primers (Takara Bio, Shiga, Japan) according to the manufacturer's instructions. Reverse transcriptase–polymerase chain reaction (RT–PCR) was performed with a primer set of PAR2 forward 5′-CCTGAGTGGCACCATCC and PAR2 reverse 5′-CAGG GAGATGCCAATGGC. The size of the expected PCR product was 527 bp. PCR conditions consisted of 5 min at 97°C, followed by 40 cycles of 30 s of denaturing at 96°C, 30 s of annealing at 57°C, 30 s of extension at 72°C, with a final extension at 72°C for 10 min. The PCR product was visualized by loading a 10 μl sample on a 2% agarose gel.

Ussing-chamber experiments

Snapwell inserts on which Calu-3 cells had grown confluent were rinsed with physiological saline solution (PSS) and transferred to the modified Ussing chambers (EasyMount Chamber; Physiologic Instruments, San Diego, CA, U.S.A.) that contained PSS at 37°C. The PSS was composed of (in mM) NaCl 115, KCl 5, $MgCl_2$ 1, $CaCl_2$ 2, glucose 10, HEPES 10, and $NaHCO_3$ 25. The pH of the solution was adjusted to 7.4 (at 37°C) using NaOH before addition of $NaHCO_3$. The pH of the solution was kept at pH 7.4 when gassed with a mixture of 5% CO_2 and 95% O_2. Transepithelial potential differences (PD) from the basolateral to the apical side of the monolayer were continuously measured under open-circuit conditions by a high-impedance millivoltmeter that could function as a voltage clamp with automatic fluid resistance compensation (VCC MC2, Physiologic Instruments). Transepithelial conductance (G_t) was determined by imposing short (0.5 s) current pulses ($\Delta I = 2$–10 μA), and the corresponding changes in transepithelial voltage (ΔV) were calculated using Ohm's law ($G_t = \Delta I\ \Delta V^{-1}$). The equivalent short-circuit current (I_{eq}) was calculated as G_t PD. I_{eq} represents net charge movement across the monolayer.

Permeabilized monolayers

To investigate apical membrane Cl^- conductance, the basolateral membrane was permeabilized with the pore-forming antibiotic nystatin (100 μM) for more than 30 min. This level of nystatin was determined as the concentration at which bumetanide, an inhibitor of the basolateral Na^+–K^+–$2Cl^-$ cotransporter, had no effect on the ion current (Son *et al*., 2004). This procedure avoids the complexities associated with basolateral ion transporters and permits analyses of apical membrane Cl^- conductance (Devor *et al*., 1999; Ito *et al*., 2002; Son *et al*., 2004). Apical membrane Cl^- conductance was estimated as apical membrane Cl^- current (I_{Cl}) in the apical-to-basolateral Cl^- concentration gradient under closed-circuit conditions. The Cl^- concentration gradient was established by

replacing NaCl with equimolar Na-gluconate in the basolateral PSS. I_{Cl} reflects the apical Cl^- permeability through cystic fibrosis transmembrane conductance regulator (CFTR) in Calu-3 cells because the apical anion conductance is almost completely derived from CFTR channels in Calu-3 cells (Haws *et al*., 1994; Devor *et al*., 1999). To completely eliminate the component of basolateral K^+ conductance in this I_{Cl} measurement, these experiments were performed in the presence of clotimazole, an inhibitor of the human intermediate conductance Ca^{2+}-activated K^+ (hIK-1) channel. In this basolateral solution, $CaCl_2$ was increased to 4 mM to compensate for the Ca^{2+}-chelating capacity of the gluconate.

The basolateral membrane K^+ conductance was estimated by measuring the basolateral membrane K^+ current (I_K) after permeabilization of the apical membrane with nystatin (50 μM) for 30 min and establishment of an apical-to-basolateral K^+ concentration gradient (Devor *et al*., 1999; Son *et al*., 2004). Complete permeabilization of the apical membrane with 50 μM nystatin was confirmed by apical application of phlorizin, an inhibitor of the Na^+-glucose transporter located on the apical membrane of this cell line (Ito *et al*., 2001; Son *et al*., 2004). Apical NaCl was replaced by equimolar K-gluconate, while basolateral NaCl was substituted with equimolar Na-gluconate. Cl^- was removed from these solutions to completely eliminate the component of apical Cl^- conductance. On the basolateral membrane, the major K^+ conductance was produced by the hIK-1 channel in Calu-3 cells (Devor *et al*., 1999; Cowley & Linsdell, 2002).

Cytosolic Ca^{2+} mobilization assay

Calu-3 cells grown on the porous membranes of Transwell inserts (Costar) were rinsed twice with PSS and incubated for 1.5 h at 37°C in the same buffer containing 5 μM fluo-3/AM (Dojindo, Kumamoto, Japan) and 0.01% pluronic F127 (Molecular Probes, Eugene, OR, U.S.A.). After the loading, cell monolayers were rinsed twice with PSS to wash off residual dyes outside the cells, and then 0.5 ml and 1 ml PSS were added to the apical and basolateral membranes, respectively. Fluorescence signals were collected for 20 ms at 6 s intervals using a fluorometer (Fluoroskan Ascent CF; Labsystems, Helsinki, Finland) at the excitation wavelength of 485 nm and the emission wavelength of 538 nm. The maximum signal (F_{max}) was obtained by addition of 10 μM ionomycin, and the minimum signal (F_{min}) was obtained by adding 10 mM EGTA to the cell monolayer. The cytosolic Ca^{2+} concentration ($[Ca^{2+}]_i$) was calculated according to the following formula:

$$[Ca^{2+}]_i(\text{nM}) = K_d(F - F_{min})(F_{max} - F)^{-1}$$

in which the K_d was assumed to be 390 nM (Minta *et al*., 1989). In the present study, maximum $[Ca^{2+}]_i$ changes ($\Delta[Ca^{2+}]_i$) were compared between groups.

Chemicals

Forskolin, isoproterenol, 1-ethyl-2-benzimdazolinone (1-EBIO), bumetanide, clotrimazole, ATP, ADPβS, adenosine, D609, nystatin, trypsin, thrombin, thapsigargin, U73122, and GF109203X were obtained from Sigma-Aldrich Co. Xestospongin C and ET-18-OCH_3 were purchased from Calbiochem (La Jolla, CA, U.S.A.). Soybeans trypsin inhibitor was from Worthington (Lakewood, NJ, U.S.A.). SLIGKV-NH_2 (a PAR2-activating peptide: PAR2AP), was a product of Bachem (Bubendorf, Switzerland). VKGILS-NH_2 (a reverse sequence peptide of PAR2AP: revPAR2AP) was synthesized by Sawady Technology Co., Ltd (Tokyo, Japan). Stock solutions of ATP, ADPβS, trypsin, thrombin, and the soybean trypsin inhibitor were prepared by dissolution in distilled water. All other drugs were dissolved in DMSO. Nystatin stock solution (100 mM) was made and sonicated for 30 s just before use.

Data analysis

Numerical data are presented as means ± s.e.m., where n refers to the number of experiments. Statistical differences were determined by Student's t-test for comparison of data between two groups or one-way analysis of variance for multiple group comparison. A value of $P<0.05$ was considered statistically significant.

Results

Bioelectric responses to PAR-related activators

Previous investigations have found that PAR2 are unilaterally located on the basolateral membrane in native airway epithelial tissues (Kunzelmann *et al*., 2002) and cultured bronchial epithelial cells (Danahay *et al*., 2001). Thus, we first applied various PAR activators to the basolateral face of the Calu-3 monolayer (Figure 1). Application of a PAR2, -4 activator, trypsin (50 U ml^{-1}), led to a rapid increase in apical side-negative PD from the baseline (-5.0 ± 0.2 mV, $n=41$) to a peak (-15.8 ± 0.5 mV), followed by a decay back to the baseline in a couple of minutes (Figure 1a). The corresponding values of I_{eq} are shown in Figure 1b. The peak values of I_{eq} (54.2 ± 1.8 μA cm^{-2}) minus basal ones (11.4 ± 0.3 μA cm^{-2}), which are expressed as ΔI_{eq}, were 42.8 ± 1.8 μA cm^{-2}. The effects of trypsin (basolateral) were interrupted by the basolateral presence of a soybean trypsin inhibitor (data not shown). In contrast to the trypsin-induced responses, thrombin (50 U ml^{-1}), a PAR1, -3, -4 activator, failed to induce any bioelectric effect on the monolayer (Figure 1c and d), suggesting expression of PAR2 exclusively on the basolateral membrane. The trypsin-induced responses were mimicked by PAR2AP: SLIGKV-NH_2, which is a short synthetic peptide with proteolytically revealed PAR2 sequences (Figure 1e and f). Basolateral application of PAR2AP (50 μM) induced a transient increase in apical side-negative PD ($\Delta PD = 22.1\pm0.8$ mV, $n=77$; Figure 1e), resulting in transient elevation of I_{eq} ($\Delta I_{eq} = 147.0\pm6.9$ μA cm^{-2}; Figure 1f). Also, the trypsin-induced responses were almost completely suppressed in the presence of PAR2AP ($\Delta I_{eq} = 5.5\pm0.8$ μA cm^{-2}, $n=4$, $P<0.001$), suggesting that trypsin and PAR2AP share a common receptor. Further, PAR2 specificity in the bioelectric responses was confirmed by the finding that the reverse sequence peptide of PAR2AP (revPAR2AP, 100 μM) had no effect on the PD and I_{eq} (Figure 1g and h).

Compared with the responses to basolateral trypsin, those to apical trypsin were small (Figure 2a). The small change made by apical trypsin was not due to its leakage to the basolateral side because a soybean trypsin inhibitor (50 U ml^{-1}) applied to the basolateral solution made no significant difference in

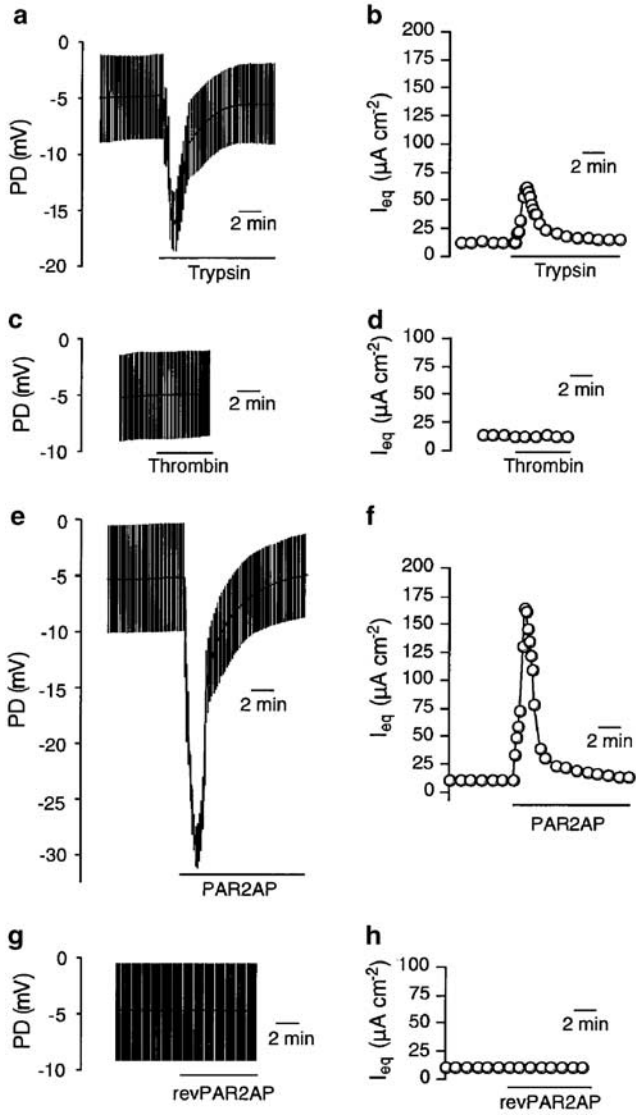

Figure 1 Representative traces of bioelectric responses to PAR activators in Calu-3 monolayer. Potential differences from the basolateral to apical side (PD) were monitored under an open-circuit condition with applications of repeated short (0.5 s) current pulses (10 μA). From the changes in PD, the equivalent short-circuit current (I_{eq}) was caluculated by Ohm's law. The cells were exposed to trypsin (50 U ml^{-1}, a and b), thrombin (50 U ml^{-1}, c and d), a PAR2-activating peptide (PAR2AP, 50 μM, e and f), and the reverse sequence peptide of PAR2AP (revPAR2AP, 50 μM, g and h) from the basolateral side.

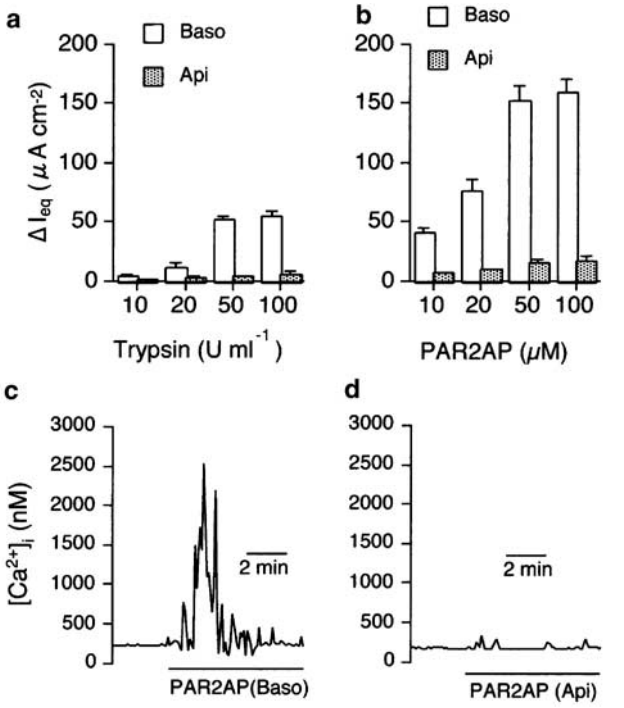

Figure 2 Comparison of effects of basolateral (Baso) and apical (Api) applications of PAR2 agonists, trypsin (a) and PAR2AP (b), at various concentrations. The ΔI_{eq} was obtained by calculating the difference between peak values after the addition of PAR2 agonists and values just before their addition. Data are means $\pm$ s.e.m. ($n=4$). (c, d) Representative tracings of $[Ca^{2+}]_i$ changes during exposure to PAR2AP from the basolateral (c) and apical side of the monolayer (d).

responses to apical trypsin at 50 U ml^{-1}: $\Delta I_{eq} = 5.1 \pm 0.8\ \mu A\ cm^{-2}$ ($n=6$) without and $5.4 \pm 0.3\ \mu A\ cm^{-2}$ ($n=4$) with 50 U ml^{-1} soybean trypsin inhibitor. Similarly, apically applied PAR2AP induced only a small effect on the responses ($\Delta I_{eq} = 14.7 \pm 3.2\ \mu A\ cm^{-2}$, $n=4$, Figure 2b), as was the case of trypsin. Figure 2c and d show cytosolic Ca^{2+} changes induced by basolateral and apical PAR2AP applications, indicating the consistency of PAR2-mediated ion transport with Ca^{2+} mobilization.

The PAR2-mediated I_{eq} almost completely comprises the Cl^- secretory component because PAR2AP-induced responses were abolished by removal of Cl^- from the extracellular solutions ($\Delta I_{eq} = 13.3 \pm 1.9\ \mu A\ cm^{-2}$, $n=4$) and the presence of basolateral bumetanide (50 μM), a Na^+–K^+–2Cl^- cotransport inhibitor ($\Delta I_{eq} = 23.2 \pm 0.8\ \mu A\ cm^{-2}$, $n=4$).

Molecular evidence of PAR2 expression

To examine PAR2 mRNA expression in Calu-3 cells, we analyzed total RNA *via* RT–PCR, which was performed using primers specific to the sequence of human PAR2. A 527-bp fragment was obtained, which was verified to be a PAR2 fragment by sequencing (Figure 3). PAR2 expression was also detected in normal human airway epithelial cells (NHBE; see Figure 3).

Potential mechanisms underlying PAR2-induced Cl^- secretion

G protein-coupled phospholipase C (PLC) is a major upstream enzyme to cause $[Ca^{2+}]_i$ mobilization and diacylglycerol (DAG)-mediated PKC activation (Hurley & Grobler, 1997). To examine the involvement of PLC in the PAR2-mediated Cl^- secretion, PD changes in response to PAR2 activators were observed in the presence of specific PLC inhibitors. Compared with the control (Figure 4a), PAR2AP (50 μM)-induced bioelectric responses in cells that had been exposed beforehand to phosphatidylinositol-phospholipase C (PI-PLC) inhibitors U73122 (100 μM Figure 4b) or ET-18-OCH_3 (100 μM) were still intact. Namely, ΔPD and ΔI_{eq} values

generated by the application of PAR2AP in the control (22.3 ± 1.4 mV and $162.3 \pm 19.0\,\mu A\,cm^{-2}$, $n=7$) were unaffected by U73122 (21.4 ± 1.2 mV and $153.0 \pm 12.0\,\mu A\,cm^{-2}$, $n=5$) and ET-18-OCH_3 (22.4 ± 1.6 mV and $163.6 \pm 26.5\,\mu A\,cm^{-2}$, $n=5$), respectively (Figure 4f). Further, PAR2-induced responses were also insensitive to (Xest C, 10 μM), a selective antagonist of inositol 1,4,5-triphosphate (Ins P_3; $\Delta PD = 21.2 \pm 2.3$ mV; $\Delta I_{eq} = 140.5 \pm 21.2\,\mu A\,cm^{-2}$, $n=5$, Figure 4c). Similar pharmacological properties were reproduced in the cells stimulated by trypsin (data not shown). In contrast to these observations, pretreatment with a specific phosphatidylcholine-phospholipase C (PC-PLC) antagonist, D609 (100 μM), markedly prevented PAR2AP-mediated PD changes ($\Delta PD = 3.9 \pm 0.5$ mV, $n=5$) and the resultant I_{eq} ($\Delta I_{eq} = 28.1 \pm 5.3\,\mu A\,cm^{-2}$, $P<0.001$), as demonstrated in Figure 4d. Figure 4e shows that the cells also became less responsive to PAR2AP in the presence of a PKC activator, PMA (1 μM): $\Delta PD = 9.6 \pm 0.9$ mV; $\Delta I_{eq} = 51.0 \pm 2.8\,\mu A\,cm^{-2}$ ($n=4$, $P<0.005$). Summarized data of each ΔI_{eq} value is shown in Figure 4f.

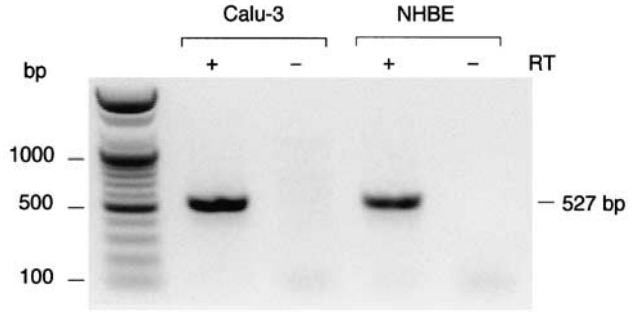

Figure 3 Products of RT–PCR of RNA isolated from Calu-3 human airway cell line and normal human bronchial epithelial cells (NHBE), using gene-specific primer pairs targeted to PAR2. A 527-bp fragment of PAR2 was obtained from these two types of cells with reverse transcription (RT) of total RNA (+) but not without RT (–).

Auto-desensitization induced by PAR2 activation

After completion of transient reactions due to PAR2AP (50 μM, basolateral), additional PAR2 stimulation (PAR2AP, 50 μM, basolateral) in the continuous presence of PAR2AP hardly generated responses (Figure 5a). The desensitization was not counteracted by pretreatment with the PKC inhibitor GFX (1 μM, Figure 5b). Figure 5c is a summary of the experiments shown in Figure 5a and b, indicating that the I_{eq} induced by the second PAR2AP application was $13.3 \pm 2.2\%$ ($n=4$) of the first one in the control, and $11.3 \pm 1.4\%$ ($n=4$) in the presence of GFX. When PAR2AP was removed after being present for 10 min, cells had only partially recovered their responsiveness to PAR2AP even 30 min later (Figure 5d),

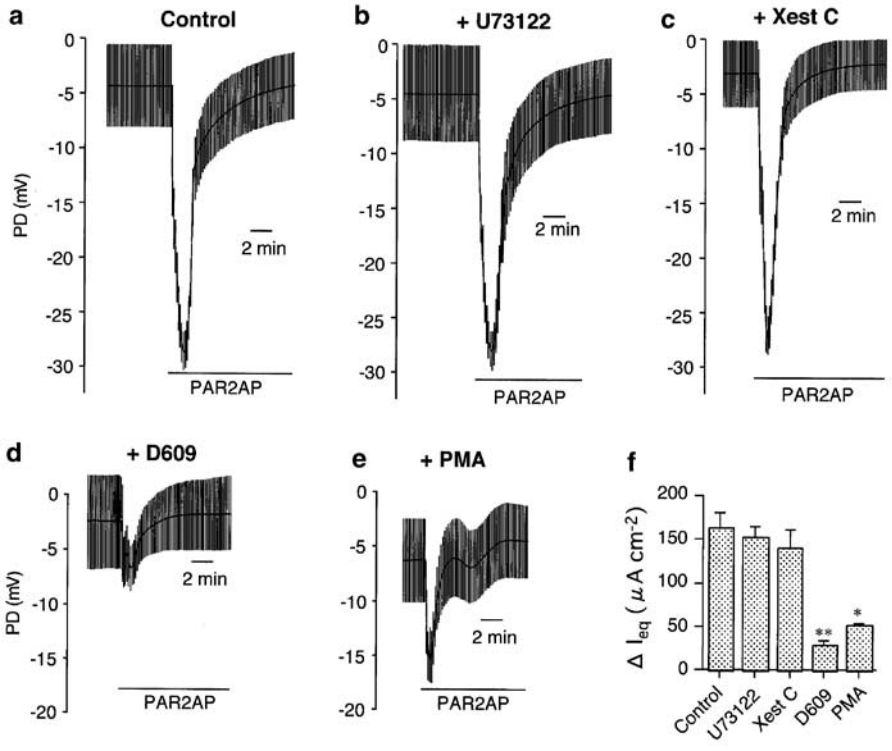

Figure 4 Mechanisms underlying PAR2-mediated anion secretion in Calu-3 cells. (a–e) Representative traces of potential differences from the basolateral to the apical side (PD) before and after application of the PAR2-activating peptide (PAR2AP, 50 μM, in the presence of the vehicle (0.1% DMSO: Control, a), U73122 (100 μM, b), xetospongin C (Xest C, 10 μM, c), D609 (100 μM, d), and PMA (1 μM, e). PD was monitored under open-circuit condition with applications of repeated short (0.5 s) current pulses (10 μA). (f) Summary of the PAR2AP-induced elevation of the equivalent short-circuit current (ΔI_{eq}), which was calculated by PD data. U73122, Xest C, D609, and PMA were applied 30 min prior to addition of PAR2AP. Data are means ± s.e.m. ($n=4$–7). *$P<0.005$, **$P<0.001$.

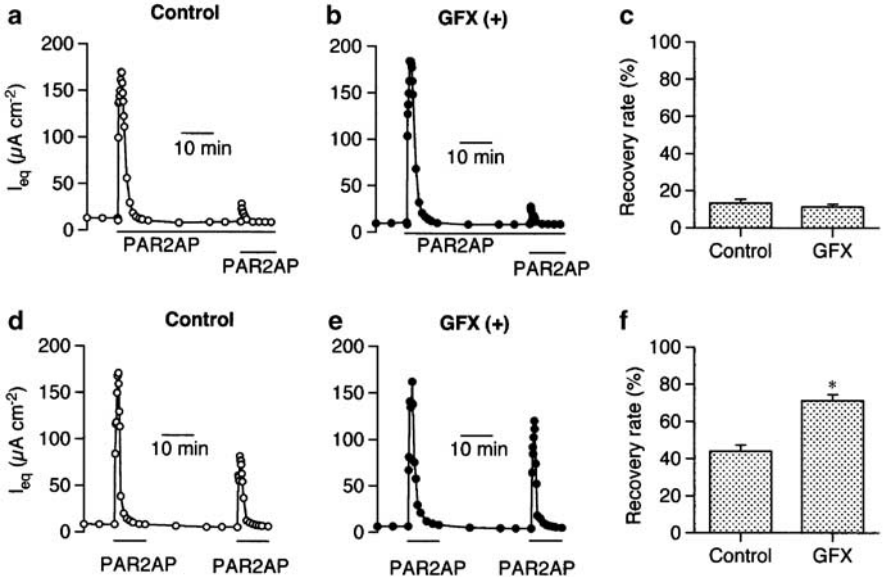

Figure 5 Auto-desensitization of PAR2-mediated signals in Calu-3 cells. (a–c) In the continuous presence of PAR2AP (50 μM, basolateral), I_{eq} responses to additional PAR2AP (50 μM, basolateral) were severely suppressed (a), and the suppression was not counteracted by the presence of the PKC inhibitor GF109203X (GFX, 1 μM, b). (c) Summary of the experiments shown in (a) and (b). Recovery rates (ordinates) were obtained by dividing the second ΔI_{eq} by the first one. (d–f) PAR2AP was removed after 10 min exposure, and PAR2AP was reapplied 30 min after its removal in the absence (d) and presence of GF109203X (GFX, 1 μM, e). (f) Summary of the experiments shown in (d) and (e). GF109203X was applied 30 min before the first application of PAR2AP. Data are means $\pm$ s.e.m. ($n=4$). *$P<0.005$, significantly different from the control values.

suggesting the desensitization remained for a long time after the wash-out. In contrast to the results shown in Figure 5a–c, however, the recovery in this case was further potentiated by the presence of GFX (Figure 5e): the responses to the second application was $43.9\pm3.5\%$ ($n=4$) of the response to the first in the control and $71.1\pm3.4\%$ ($n=4$, $P<0.005$) in the presence of GFX (Figure 5f).

Cross-desensitization caused by PAR2 activation

Next, we observed the effect of PAR2 stimulation on responses to various anion secretagogues. As shown in Figure 6a–d, I_{eq} responses to isoproterenol (10 nM, a β-adrenergic agonist), forskolin (10 μM, an adenylate cyclase (AC) activator), thapsigargin (1 μM, a Ca^{2+} mobilizing agent due to inhibition of Ca^{2+}-ATPase and stimulation of capacitative Ca^{2+} entry), 1-EBIO (1 mM, a direct opener of human intermediated conductance, inward-rectifying Ca^{2+}-activated K^+ [hIK-1] channels) were unaffected by pretreatment with PAR2AP (50 μM, for 30 min). After PAR2 pretreatment, however, the cells became less responsive only to ATP (Figure 6e) and ADPβS. Namely, ΔI_{eq} produced by ATP (100 μM, apical) and ADPβS (100 μM, apical) were reduced from 46.6 ± 3.7 μA cm^{-2} ($n=10$) and 32.9 ± 1.4 μA cm^{-2} ($n=19$) to 16.6 ± 1.5 μA cm^{-2} ($n=8$, $P<0.001$) and 19.4 ± 1.6 μA cm^{-2} ($n=4$, $P<0.001$), respectively. In contrast, responses to an A_{2B} agonist, adenosine, a metabolite of ATP through ectonucleotidases, were intact in the presence of PAR2AP (Figure 6f).

It was previously reported that extracellular ATP and ADPβS cause Cl^- secretion *via* $P2Y_1$ purinoceptor ($P2Y_1R$), which is coupled both to AC and PC-PLC in Calu-3 cells (Communi *et al*., 1999; Son *et al*., 2004). Thus, there are three possible explanations for the attenuation of $P2Y_1R$-mediated Cl^- secretion: the stimulation of PAR2 inhibits (1) the AC/cAMP pathway relevant to CFTR activities, (2) the PC-PLC-Ca^{2+} pathway regulating the basolateral hIK-1 channel that provides a driving force for Cl^- secretion, or (3) both. To rule out the involvement of cAMP-dependent signal transductions in the PAR2-induced suppression of $P2Y_1R$ signals, apical membrane Cl^- conductance, which reflects CFTR (a cAMP-dependent Cl^- channel)-mediated anion conductance, was followed by apical application of extracellular ATP (100 μM) under nystatin-permeabilized conditions (Figure 7a and b). However, the presence of PAR2AP (50 μM, Figure 7b) failed to affect the inward I_{Cl} across the apical membrane in the apical to basolateral Cl^- gradient (Figure 7b). Indeed, there was no significant difference in the ATP-augmented ΔI_{Cl} between the groups with PAR2AP (43.9 ± 3.0 μA cm^{-2}, $n=4$) and without (41.7 ± 4.4 μA cm^{-2}). In contrast, an ATP-induced increase in basolateral membrane I_K ($\Delta I_K=28.2\pm0.7$ μA cm^{-2}, $n=4$, Figure 7c), which is highly sensitive to charybdotoxin, a selective hIK-1 inhibitor (Son *et al*., 2004), was significantly reduced by the pretreatment with PAR2AP ($\Delta I_K=14.7\pm0.6$ μA cm^{-2}, $n=4$, $P<0.001$, Figure 7d).

In addition, fluo-3 signal measurement revealed that apically applied ATP (100 μM) elevated $[Ca^{2+}]_i$ in an oscillatory fashion (Figure 8a). The ATP-induced $[Ca^{2+}]_i$ changes were markedly attenuated by the presence of D609 (a PC-PLC inhibitor) or PMA (a PKC activator), and were also suppressed by the PAR2AP pretreatment (Figure 8b–d). Namely, $\Delta[Ca^{2+}]_i$ was reduced from 1288.5 ± 356.2 nM ($n=9$, Figure 8a) to 178.1 ± 51.2 nM ($n=6$, $P<0.05$, Figure 8d) by the presence of PAR2AP. Further, the PAR2-mediated attenuation of $[Ca^{2+}]_i$ movement was reversed by the PKC inhibitor GFX (1 μM) up to 423.8 ± 59.9 nM ($n=6$, $P<0.05$ vs without GFX, Figure 8e).

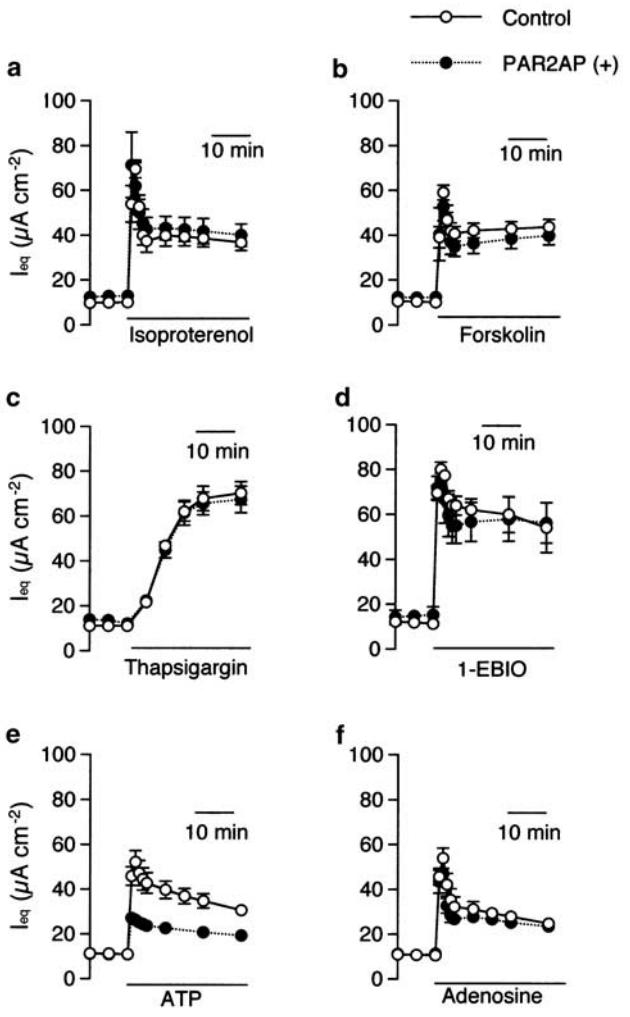

Figure 6 PAR2-induced desensitization of the subsequent heterologous responses. I_{eq} responses to isoproterenol (10 nM, basolateral, a), forskolin (10 μM, basolateral, b), thapsigargin (1 μM, apical, c), and 1-ethyl-2-benzimdazolinone (1-EBIO, 1 mM, bilateral, d) were unaffected by pretreatment with PAR2AP (PAR2AP (+), 50 μM, basolateral) applied 30 min prior to these anion secretagogues. In contrast, ATP-induced I_{eq} was inhibited by the presence this PAR2 agonist (e), although the responses to adenosine, a metabolite of ATP through ectonucleotidases, were intact under this condition (f). Data are means ± s.e.m. ($n = 4$–12).

Discussion

Thrombin (a PAR1, -3, -4 agonist) and trypsin (a PAR2, -4 agonist) are well-characterized enzymatic activators of PARs (Dery *et al*., 1998). We showed in human airway epithelial Calu-3 cells that trypsin, but not thrombin, applied to the basolateral face of the monolayer caused a transient change in ion transport that was mimicked by the application of PAR2AP, suggesting selective PAR2 expression. Our RT–PCR experiments to detect PAR2 mRNA verified this point in the present study. When trypsin and PAR2AP were used to determine concentration-dependent responses, apical application of these PAR2 agonists caused much smaller effects than basolateral application did. These observations indicate predominant localization of PAR2 on the basolateral membrane of Calu-3 cells, in accordance with native and cultured airway epithelial cells (Danahay *et al*., 2001; Kunzelmann *et al*., 2002). The most likely second messenger in the regulation of PAR2-mediated ion transport is cytosolic Ca^{2+}, because PAR2-mediated I_{eq} changes were well correlated to those in $[Ca^{2+}]_i$, as has been reported in normal human airway epithelial cells (Danahay *et al*., 2001). Calu-3 cells display the phenotype of CFTR-rich airway epithelium without any component of amiloride-sensitive Na^+ absorption, and $[Ca^{2+}]_i$ elevation causes Cl^- secretion but neither HCO_3^- secretion nor Na^+ absorption (Moon *et al*., 1997; Singh *et al*., 1997; Devor *et al*., 1999). This would render it conceivable that PAR2-stimulated ion transport in Calu-3 cells essentially comprises Cl^- secretion. This speculation was confirmed by the results that PAR2AP-induced responses were markedly suppressed by removal of Cl^- from the extracellular solutions and the presence of basolateral bumetanide, an inhibitor of Cl^- uptake across the basolateral membrane *via* the Na^+–K^+–$2Cl^-$ cotransporter. Although Calu-3 cells almost exclusively express CFTR without Ca^{2+}-dependent Cl^- channels (Haws *et al*., 1994), Ca^{2+}-dependent CFTR-mediated Cl^- secretion does occur. Namely, activation of basolateral Ca^{2+}-activated K^+ channels provides a driving force for Cl^- efflux across the apical CFTR at rest (Moon *et al*., 1997). In Calu-3 cells, the majority of basolateral K^+ conductance can be accounted for by the hIK-1 channel (an intermediate conductance Ca^{2+}-activated K^+ channel) because only a small cAMP-activated K^+ conductance but a much larger hIK-1-dependent K^+ conductance could be identified in the permeabilized monolayer (Devor *et al*., 1999; Cowley & Linsdell, 2002; Ito *et al*., 2004b; Szkotak *et al*., 2004). Preliminarily, we ascertained that PAR2-induced I_{eq} was significantly inhibited by the hIK-1 channel inhibitors charybdotoxin and clotrimazole (data not shown). Thus, it is most likely that PAR2-induced Cl^- secretion *via* resting CFTR is generated by Ca^{2+}-dependent activation of the basolateral hIK-1 channel (see Figure 7b and d).

In most cellular systems, the key enzyme for the regulation of intracellular Ca^{2+} mobilization is G protein-coupled PLC. PLC is classified into PI-PLC and PC-PLC (Camina *et al*., 1999). PI-PLC stimulates the breakdown of phosphatidylinositol 4,5-biphosphate at the internal leaflet of the plasma membrane to form two second messengers, $InsP_3$ and DAG (Nakamura, 1996). $InsP_3$ triggers Ca^{2+} release from the endoplasmic reticulum, while DAG activates transient receptor potential channels, Ca^{2+} entry pathways (Kiselyov & Muallem, 1999). There are several lines of evidence that PAR-mediated Ca^{2+} mobilization is coupled to PI-PLC (Mule *et al*., 2002; Oshiro *et al*., 2002). Nevertheless, the results in Figure 4 revealed that the PAR2-mediated responses were unaffected by PI-PLC inhibitors, such as U73122 ($K_i = 4$–10 μM) (Connor *et al*., 2001; Saeed *et al*., 2003; Rasheed & Saeed, 2004) or ET-18-OCH_3 ($K_i = 2$–18 μM) (Powis *et al*., 1992; Daniel *et al*., 1995; Seebeck *et al*., 1998), and an $InsP_3$ inhibitor, Xest C ($K_i = 0.3$–0.4 μM) (Gafni *et al*., 1997). However, recent studies have shed light on PC-PLC as an alternative pathway for production of DAG (Snetkov *et al*., 2001). In the present study, PAR2AP-induced Cl^- secretion and Ca^{2+} mobilization were markedly diminished by pretreatment with a specific PC-PLC inhibitor (D609), whose K_i on PC-PLC has been reported to be 5–20 μM (Tschaikowsky *et al*., 1994; Amtmann, 1996;

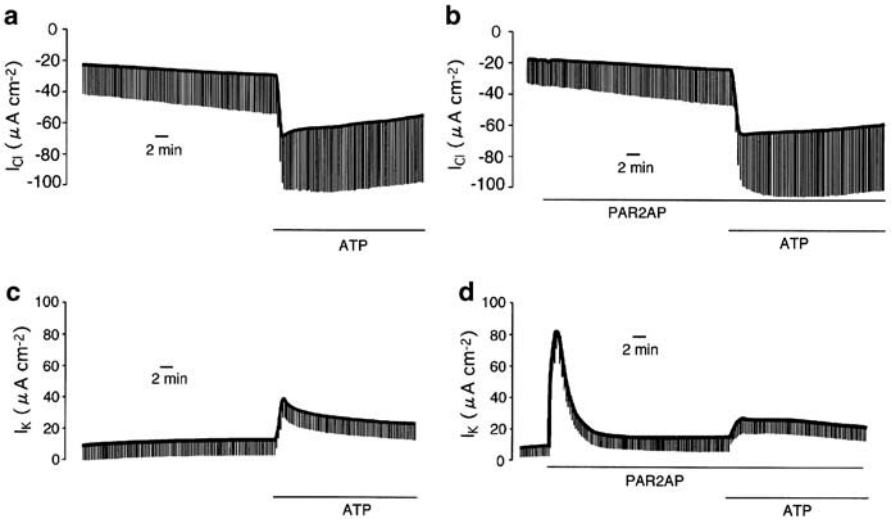

Figure 7 (a, b) Effects of PAR2 activation on extracellular ATP-induced Cl^- conductance across the apical membrane in nystatin-permeabilized Calu-3 monolayer (see Methods). To isolate apical Cl^- conductance, the apical membrane Cl^- current (I_{Cl}) was measured after the apical to basolateral Cl^- gradient was established. An inward I_{Cl} is consistent with an absorptive Cl^- flow. (a) Under this condition, Cl^- conductance was continuously augmented by ATP (100 μM) added to the apical solution. (b) Even in the cells pretreated with PAR2AP (50 μM), the ATP-induced Cl^- conductance was not significantly affected. (c, d) Effects of PAR2 activation on ATP-induced K^+ conductance across the basolateral membrane in a nystatin-permeabilized Calu-3 monolayer (see Methods). Basolateral membrane K^+ conductance was estimated through basolateral membrane K^+ current after establishment of an apical-to-basolateral K^+ gradient. (c) K^+ conductance was increased by additon of ATP (100 μM) to the apical solution. (d) Application of PAR2AP induced a transient increase in I_K. After exposure to PAR2AP (50 μM, basolateral) for 30 min, an ATP-induced increase in K^+ conductance was attenuated. These experiments were performed under closed-circuit conditions.

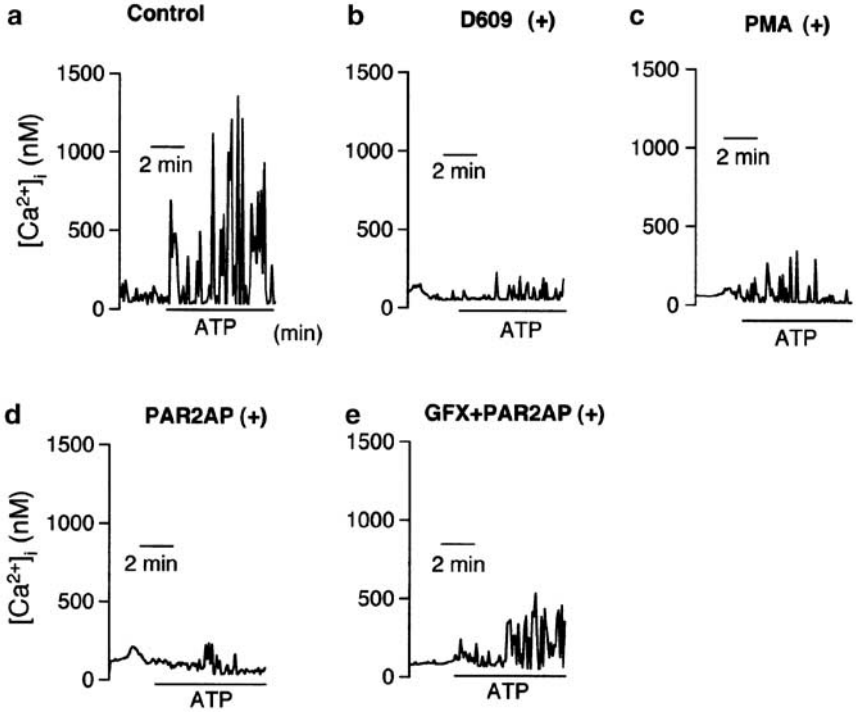

Figure 8 (a–e) Effects of PARAP2 on extracellular ATP-induced Ca^{2+} mobilization in Calu-3 cells preloaded with fluo-3. Application of ATP (100 μM, apical) on the apical side increased $[Ca^{2+}]_i$ in a oscillatory fashion (a). The ATP-induced Ca^{2+} mobilization, which was significantly suppressed by D609 (100 μM, b) or PMA (1 μM, c), was also abolished by pretreatment with the PAR2-activating peptide (PAR2AP, 50 μM, basolateral, d). The PAR2-mediated attenuation was blunted by pretreatment with the PKC inhibitor GF109203X (GFX, 1 μM, e). D609, PMA, PAR2AP, and GF109203X were applied 30 min before addition of ATP.

Kengatharan *et al*., 1996; Nakahata *et al*., 2000). These results, thereby, suggest the possible coupling of PAR2 with PC-PLC on the basolateral membrane of Calu-3.

PAR-mediated activation of PC-PLC and resultant generation of DAG should activate PKC as well as mobilize Ca^{2+} (Nystedt *et al*., 1994). PKC has been reported to be involved in

regulating PAR2-mediated Ca^{2+} mobilization in kidney and intestinal epithelial cell lines (Bohm *et al*., 1996). To investigate the effect of PKC on PAR2-mediated Cl^- secretion in Calu-3 cells, cells pretreated with PMA, a PKC activator, were exposed to PAR2AP, showing that PAR2 on Calu-3 cells seem likely to be under the regulation of PKC (see Figure 4e and f). From these observations, we predicted that PKC activation *via* PAR2 stimulation is involved in its auto-desensitization, and consequently we found it partially involved. To put it concretely, auto-desensitization during the continuous exposure to PAR2AP, however, was unaffected by a PKC inhibitor (Figure 5a and b), whereas auto-desensitization during the intermittent exposure to PAR2AP was mitigated by the PKC inhibition (see Figure 5d and e). In other words, PAR2-mediated PKC activation participates in extension of PAR2 auto-desensitization even after recovery from PKC-independent auto-desensitization (i.e., uncoupling from G-protein, or internalization into early endosomes) (Dery *et al*., 1998; Macfarlane *et al*., 2001).

PKC could be implicated in cross-desensitization between different receptors, supposing auto-desensitization of PAR2 involves PKC, which may act at the level of the receptor or at more distal steps in the signaling pathway (Bohm *et al*., 1996). Thus, we examined the effects of PAR2 activation on the anion secretion due to heterologous stimuli in Calu-3 cells. As shown in Figure 6, anion secretion generated by cAMP-related agents, such as isoproterenol, forskolin, and adenosine, were unaffected by the PAR2 activation through PAR2AP, suggesting that PAR2 activation does not influence signals *via* AC-coupled receptors (i.e., β_2-adrenergic receptor, A_{2B} adenosine receptor), the cAMP-PKA cascade, and cAMP-dependent channels (i.e., CFTR, cAMP-dependent K^+ channels). Thapsigargin inhibits the Ca^{2+}-ATPase that contributes to the Ca^{2+} uptake of intracellular Ca^{2+} into its store sites, leading to $[Ca^{2+}]_i$ elevation (Kim *et al*., 1998). Depletion of Ca^{2+} in the store sites due to thapsigargin also stimulates Ca^{2+} entry from the extracellular space (Takemoto *et al*., 1998). $[Ca^{2+}]_i$ elevation causes an opening of the basolateral hIK-1 channel, leading to Cl^- secretion, as described above. Thus, to determine whether Ca^{2+} mobilization itself or the hIK-1 channel was a target of PAR2-mediated desensitization, we examined the effects of PAR2 activation on the thapsigargin- and 1-EBIO (a hIK-1 opener)-induced anion secretion, but found no significant effect. Notwithstanding these observations, we found in this study that ATP- and ADPβS-induced anion secretion was desensitized by the pretreatment with PAR2AP. Previous studies to detect subtypes of P2Y receptors revealed that only $P2Y_1R$ mRNA is expressed in Calu-3 cells (Communi *et al*., 1999), and extracellular ATP and ADPβS is well capable of stimulating this purinoceptor (Ralevic & Burnstock, 1998; Son *et al*., 2004). We have previously demonstrated that stimulation of $P2Y_1R$, which is coupled to both AC and PC-PLC, simultaneously causes CFTR activation and Ca^{2+} mobilization, generating Cl^- secretion (Son *et al*., 2004). The locus of the $P2Y_1R$-mediated signal transduction affected by PAR2 activation is not at the receptor levels but in the stream of the PC-PLC-mediated pathway, because, as shown in Figures 7 and 8, CFTR-mediated apical Cl^- conductance augmented by the addition of ATP was unchanged under PAR2-prestimulated conditions, while pretreatment with PAR2AP markedly attenuated ATP-mediated Ca^{2+} mobilization and elevation of basolateral K^+ conductance that is predominantly mediated by a Ca^{2+}-activated K^+ channel hIK-1 in Calu-3 cells (Son *et al*., 2004). Further, the PAR2-mediated inhibition of ATP-induced Ca^{2+} mobilization was counteracted by the presence of a PKC inhibitor GFX. Therefore, we conclude that PC-PLC-mediated PKC activation through PAR2 causes a selective cross-desensitization of the $P2Y_1R$–PC-PLC pathway.

Of the PAR2-mediated auto-and cross-desensitizations, PKC activation *via* PC-PLC may act on G proteins, PC-PLC, or later steps in the signaling pathway. Nevertheless, it is more likely that G-proteins are not a principal target of PKC because of the previous findings that the G_{q2}-subunit, which is at least partially involved in PAR2- and $P2Y_1$-transduction (Ralevic & Burnstock, 1998; Macfarlane *et al*., 2001), is not phosphorylated by PMA (Lounsbury *et al*., 1993). Further, it has been reported that thapsigargin-induced Ca^{2+} mobilization, which acts on distal steps in the PLC pathway, is insensitive to PMA (Munshi *et al*., 1993), suggesting less involvement of PKC in the distal steps of PC-PLC. Add results

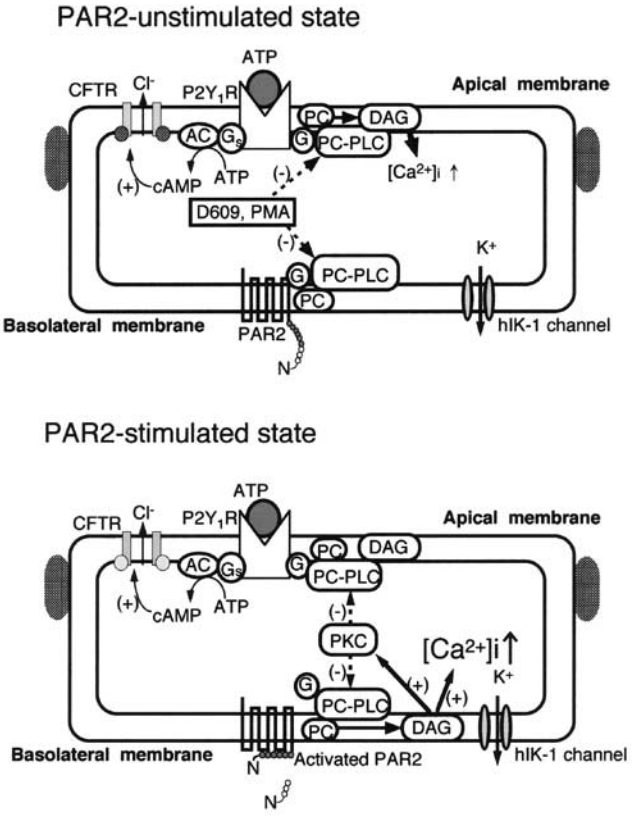

Figure 9 Possible mechanisms underlying PAR2-mediated desensitization related to PKC in Calu-3 cells. (+) and (−) indicate stimulatory and inhibitory effects, respectively. Both basolateral PAR2 and apical $P2Y_1$ purinoceptor ($P2Y_1R$) are coupled with PC-PLC, which hydrolyzes phosphatidylcholine at the plasma membrane. PC-PLC activity is inhibited by D609 and PMA. PAR2-mediated PC-PLC activation and the resultant formation of DAG are greatly responsible for Ca^{2+} mobilization, which activates the basolateral hIK-1 channel for Cl^- secretion, and PKC activation, which inhibits PC-PLC activity. The PAR2-mediated PKC activation leads to desensitization of PAR2 itself and $P2Y_1R$ through PKC-to-PC-PLC negative feedback mechanisms. In this process, the adenylate cyclase (AC)-mediated pathway, which is also coupled with $P2Y_1R$, is intact.

shown in Figure 6c is also suggestive regarding this point. Alternatively, PC-PLC seems more likely to be a target for PAR2-mediated, PKC-dependent desensitization because both PC-PLC and PI-PLC are phosphorylated in response to activation of PKC by the PKC activator PMA or through PLC-coupled receptors, preventing interaction with G_i- and G_q-proteins (Camina *et al*., 1999). Considering the results obtained from the present study, we propose the hypothetical scheme of PAR2-mediated regulation of $P2Y_1R$ shown in Figure 9.

In conclusion, PAR2 stimulation generates a brief response of Cl^- secretion through PC-PLC-mediated pathway, followed by not only auto-desensitization of PAR2 itself but also cross-desensitization of a PC-PLC-coupled purinoceptor ($P2Y_1R$). In both types of desensitization, PKC-to-PC-PLC negative feedback mechanisms appear to be involved. As a corollary of these results, the auto- and cross-desensitization of PAR2 signal transduction may be one of the important systems regulating airway anion secretion.

This work was supported by Research Grant Funds from the Ministry of Education, Culture, Sports, Science and Technology of Japan, the Hibino Memorial Research Fund, and the Aichi Health Promotion Foundation to Y. Ito.

References

AIKAWA, T., SHIMURA, S., SASAKI, H., EBINA, M. & TAKISHIMA, T. (1992). Marked goblet cell hyperplasia with mucus accumulation in the airways of patients who died of severe acute asthma attack. *Chest,* **101,** 916–921.

AMTMANN, E. (1996). The antiviral, antitumoural xanthate D609 is a competitive inhibitor of phosphatidylcholine-specific phospholipase C. *Drugs. Exp. Clin. Res.,* **22,** 287–294.

BOHM, S.K., KHITIN, L.M., GRADY, E.F., APONTE, G., PAYAN, D.G. & BUNNETT, N.W. (1996). Mechanisms of desensitization and resensitization of proteinase-activated receptor-2. *J. Biol. Chem.,* **271,** 22003–22016.

CAMINA, J.P., CASABIELL, X. & CASANUEVA, F.F. (1999). Inositol 1,4,5-trisphosphate-independent Ca^{2+} mobilization triggered by a lipid factor isolated from vitreous body. *J. Biol. Chem.,* **274,** 28134–28141.

COCKS, T.M., FONG, B., CHOW, J.M., ANDERSON, G.P., FRAUMAN, A.G., GOLDIE, R.G., HENRY, P.J., CARR, M.J., HAMILTON, J.R. & MOFFATT, J.D. (1999). A protective role for protease-activated receptors in the airways. *Nature,* **398,** 156–160.

COCKS, T.M. & MOFFATT, J.D. (2000). Protease-activated receptors: sentries for inflammation? *Trends Pharmacol. Sci.,* **21,** 103–108.

COCKS, T.M. & MOFFATT, J.D. (2001). Protease-activated receptor-2 (PAR2) in the airways. *Pulm. Pharmacol. Ther.,* **14,** 183–191.

COMMUNI, D., PAINDAVOINE, P., PLACE, G.A., PARMENTIER, M. & BOEYNAEMS, J.M. (1999). Expression of P2Y receptors in cell lines derived from the human lung. *Br. J. Pharmacol.,* **127,** 562–568.

CONNOR, J.D., RASHEED, H., GILANI, A.H., CHEEMA, M., RIZVI, Z. & SAEED, S.A. (2001). Second messengers in platelet aggregation evoked by serotonin and A23187, a calcium ionophore. *Life Sci.,* **69,** 2759–2764.

COWLEY, E.A. & LINSDELL, P. (2002). Characterization of basolateral K^+ channels underlying anion secretion in the human airway cell line Calu-3. *J. Physiol.,* **538,** 747–757.

DANAHAY, H., WITHEY, L., POLL, C.T., VAN DE GRAAF, S.F. & BRIDGES, R.J. (2001). Protease-activated receptor-2-mediated inhibition of ion transport in human bronchial epithelial cells. *Am. J. Physiol. Cell Physiol.,* **280,** C1455–C1464.

DANIEL, L.W., CIVOLI, F., ROGERS, M.A., SMITHERMAN, P.K., RAJU, P.A. & ROEDERER, M. (1995). ET-18-OCH3 inhibits nuclear factor-kappa B activation by 12-*O*-tetradecanoylphorbol-13-acetate but not by tumor necrosis factor-alpha or interleukin 1 alpha. *Cancer Res.,* **55,** 4844–4849.

DERY, O., CORVERA, C.U., STEINHOFF, M. & BUNNETT, N.W. (1998). Proteinase-activated receptors: novel mechanisms of signaling by serine proteases. *Am. J. Physiol.,* **274,** C1429–C1452.

DEVOR, D.C., SINGH, A.K., LAMBERT, L.C., DELUCA, A., FRIZZELL, R.A. & BRIDGES, R.J. (1999). Bicarbonate and chloride secretion in Calu-3 human airway epithelial cells. *J. Gen. Physiol.,* **113,** 743–760.

GAFNI, J., MUNSCH, J.A., LAM, T.H., CATLIN, M.C., COSTA, L.G., MOLINSKI, T.F. & PESSAH, I.N. (1997). Xestospongins: potent membrane permeable blockers of the inositol 1,4,5-trisphosphate receptor. *Neuron,* **19,** 723–733.

HAWS, C., FINKBEINER, W.E., WIDDICOMBE, J.H. & WINE, J.J. (1994). CFTR in Calu-3 human airway cells: channel properties and role in cAMP-activated Cl- conductance. *Am. J. Physiol.,* **266,** L502–L512.

HURLEY, J.H. & GROBLER, J.A. (1997). Protein kinase C and phospholipase C: bilayer interactions and regulation. *Curr. Opin. Struct. Biol.,* **7,** 557–565.

INGLIS, S.K., OLVER, R.E. & WILSON, S.M. (2000). Differential effects of UTP and ATP on ion transport in porcine tracheal epithelium. *Br. J. Pharmacol.,* **130,** 367–374.

ITO, Y., NAKAYAMA, S., SON, M., KUME, H. & YAMAKI, K. (2001). Protection by tetracyclines against ion transport disruption caused by nystatin in human airway epithelial cells. *Toxicol. Appl. Pharmacol.,* **177,** 232–237.

ITO, Y., SATO, S., SON, M., KONDO, M., KUME, H., TAKAGI, K. & YAMAKI, K. (2002). Bisphenol A inhibits Cl^- secretion by inhibition of basolateral K^+ conductance in human airway epithelial cells. *J. Pharmacol. Exp. Ther.,* **302,** 80–87.

ITO, Y., SON, M., SATO, S., ISHIKAWA, T., KONDO, M., NAKAYAMA, S., SHIMOKATA, K. & KUME, H. (2004a). ATP release triggered by activation of the Ca^{2+}-activated K^+ channel in human airway Calu-3 cells. *Am. J. Respir. Cell Mol. Biol.,* **30,** 388–395.

ITO, Y., SON, M., SATO, S., OHASHI, T., KONDO, M., SHIMOKATA, K. & KUME, H. (2004b). Effects of fluoranthene, a polycyclic aromatic hydrocarbon, on cAMP-dependent anion secretion in human airway epithelia. *J. Pharmacol. Exp. Ther.,* **308,** 651–657.

KELLERMAN, D.J. (2002). $P2Y_2$ receptor agonists: a new class of medication targeted at improved mucociliary clearance. *Chest,* **121,** 201S–205S.

KENGATHARAN, M., DE KIMPE, S.J. & THIEMERMANN, C. (1996). Analysis of the signal transduction in the induction of nitric oxide synthase by lipoteichoic acid in macrophages. *Br. J. Pharmacol.,* **117,** 1163–1170.

KIM, Y.K., SAKONG, J., CHO, K.H. & LEE, C.O. (1998). Vanadate-sensitive microsomal ATPases and microsomal $45Ca^{2+}$ uptake in tracheal epithelial cells. *J. Biochem. (Tokyo),* **124,** 1094–1100.

KISELYOV, K. & MUALLEM, S. (1999). Fatty acids, diacylglycerol, $Ins(1,4,5)P_3$ receptors and Ca^{2+} influx. *Trends Neurosci.,* **22,** 334–337.

KNIGHT, D.A., LIM, S., SCAFFIDI, A.K., ROCHE, N., CHUNG, K.F., STEWART, G.A. & THOMPSON, P.J. (2001). Protease-activated receptors in human airways: upregulation of PAR-2 in respiratory epithelium from patients with asthma. *J. Allergy Clin. Immunol.,* **108,** 797–803.

KUNZELMANN, K., SCHREIBER, R., KONIG, J. & MALL, M. (2002). Ion transport induced by proteinase-activated receptors (PAR2) in colon and airways. *Cell Biochem. Biophys.,* **36,** 209–214.

LOUNSBURY, K.M., SCHLEGEL, B., PONCZ, M., BRASS, L.F. & MANNING, D.R. (1993). Analysis of Gz alpha by site-directed mutagenesis. Sites and specificity of protein kinase C-dependent phosphorylation. *J. Biol. Chem.,* **268,** 3494–3498.

LUNDGREN, J.D. & SHELHAMER, J.H. (1990). Pathogenesis of airway mucus hypersecretion. *J. Allergy Clin. Immunol.,* **85,** 399–417.

MACFARLANE, S.R., SEATTER, M.J., KANKE, T., HUNTER, G.D. & PLEVIN, R. (2001). Proteinase-activated receptors. *Pharmacol. Rev.,* **53,** 245–282.

MINTA, A., KAO, J.P. & TSIEN, R.Y. (1989). Fluorescent indicators for cytosolic calcium based on rhodamine and fluorescein chromophores. *J. Biol. Chem.,* **264,** 8171–8178.

MOON, S., SINGH, M., KROUSE, M.E. & WINE, J.J. (1997). Calcium-stimulated Cl^- secretion in Calu-3 human airway cells requires CFTR. *Am. J. Physiol.,* **273,** L1208–L1219.

MULE, F., BAFFI, M.C., FALZONE, M. & CERRA, M.C. (2002). Signal transduction pathways involved in the mechanical responses to protease-activated receptors in rat colon. *J. Pharmacol. Exp. Ther.,* **303,** 1265–1272.

MUNSHI, R., DEBERNARDI, M.A. & BROOKER, G. (1993). P2U-purinergic receptors on C_6-2B rat glioma cells: modulation of cytosolic Ca^{2+} and cAMP levels by protein kinase C. *Mol. Pharmacol.,* **44,** 1185–1191.

NAKAHATA, N., TAKANO, H. & OHIZUMI, Y. (2000). Thromboxane A_2 receptor-mediated tonic contraction is attributed to an activation of phosphatidylcholine-specific phospholipase C in rabbit aortic smooth muscles. *Life Sci.,* **66,** PL71–PL76.

NAKAMURA, S. (1996). Phosphatidylcholine hydrolysis and protein kinase C activation for intracellular signaling network. *J. Lipid Mediat. Cell Signal.,* **14,** 197–202.

NYSTEDT, S., EMILSSON, K., WAHLESTEDT, C. & SUNDELIN, J. (1994). Molecular cloning of a potential proteinase activated receptor. *Proc. Natl. Acad. Sci. U.S.A.,* **91,** 9208–9212.

OSHIRO, A., OTANI, H., YAGI, Y., FUKUHARA, S. & INAGAKI, C. (2002). Protease-activated receptor-2-mediated Ca^{2+} signaling in guinea pig tracheal epithelial cells. *Life Sci.,* **71,** 547–558.

POWIS, G., SEEWALD, M.J., GRATAS, C., MELDER, D., RIEBOW, J. & MODEST, E.J. (1992). Selective inhibition of phosphatidylinositol phospholipase C by cytotoxic ether lipid analogues. *Cancer Res.,* **52,** 2835–2840.

RALEVIC, V. & BURNSTOCK, G. (1998). Receptors for purines and pyrimidines. *Pharmacol. Rev.,* **50,** 413–492.

RAMMINGER, S.J., COLLETT, A., BAINES, D.L., MURPHIE, H., MCALROY, H.L., OLVER, R.E., INGLIS, S.K. & WILSON, S.M. (1999). $P2Y_2$ receptor-mediated inhibition of ion transport in distal lung epithelial cells. *Br. J. Pharmacol.,* **128,** 293–300.

RASHEED, H. & SAEED, S.A. (2004). Involvement of thromboxane A_2 and tyrosine kinase in the synergistic interaction of platelet activating factor and calcium ionophore A23187 in human platelet aggregation. *Exp. Mol. Med.,* **36,** 220–225.

SAEED, S.A., RASHEED, H. & GILANI, A.U. (2003). Synergism interaction between arachidonic acid by 5-hydroxytryptamine in human platelet aggregation is mediated through multiple signalling pathways. *Acta. Pharmacol. Sin.,* **24,** 958–964.

SEEBECK, J., KRUSE, M.L., SCHMIDT-CHOUDHURY, A., SCHMIDT-MAYER, J. & SCHMIDT, W.E. (1998). Pituitary adenylate cyclase activating polypeptide induces multiple signaling pathways in rat peritoneal mast cells. *Eur. J. Pharmacol.,* **352,** 343–350.

SHEN, B.Q., FINKBEINER, W.E., WINE, J.J., MRSNY, R.J. & WIDDICOMBE, J.H. (1994). Calu-3: a human airway epithelial cell line that shows cAMP-dependent Cl^- secretion. *Am. J. Physiol.,* **266,** L493–L501.

SHIMURA, S. (2000). Signal transduction of mucous secretion by bronchial gland cells. *Cell Signal,* **12,** 271–277.

SINGH, M., KROUSE, M., MOON, S. & WINE, J.J. (1997). Most basal I_{SC} in Calu-3 human airway cells is bicarbonate-dependent Cl^- secretion. *Am. J. Physiol.,* **272,** L690–L698.

SNETKOV, V.A., HAPGOOD, K.J., MCVICKER, C.G., LEE, T.H. & WARD, J.P. (2001). Mechanisms of leukotriene D_4-induced constriction in human small bronchioles. *Br. J. Pharmacol.,* **133,** 243–252.

SON, M., ITO, Y., SATO, S., ISHIKAWA, T., KONDO, M., NAKAYAMA, S., SHIMOKATA, K. & KUME, H. (2004). Apical and basolateral ATP-induced anion secretion in polarized human airway epithelia. *Am. J. Respir. Cell Mol. Biol.,* **30,** 411–419.

SZKOTAK, A.J., MURTHY, M., MACVINISH, L.J., DUSZYK, M. & CUTHBERT, A.W. (2004). 4-Chloro-benzo[F]isoquinoline (CBIQ) activates CFTR chloride channels and KCNN4 potassium channels in Calu-3 human airway epithelial cells. *Br. J. Pharmacol.,* **142,** 531–542.

TAKEMOTO, M., TAKAGI, K., OGINO, K. & TOMITA, T. (1998). Comparison of contractions produced by carbachol, thapsigargin and cyclopiazonic acid in the guinea-pig tracheal muscle. *Br. J. Pharmacol.,* **124,** 1449–1454.

TSCHAIKOWSKY, K., MEISNER, M., SCHONHUBER, F. & RUGHEIMER, E. (1994). Induction of nitric oxide synthase activity in phagocytic cells inhibited by tricyclodecan-9-yl-xanthogenate (D609). *Br. J. Pharmacol.,* **113,** 664–668.

YAMAOKA, K., MASUDA, K., OGAWA, H., TAKAGI, K., UMEMOTO, N. & YASUOKA, S. (1998). Cloning and characterization of the cDNA for human airway trypsin-like protease. *J. Biol. Chem.,* **273,** 11895–11901.

(Received February 7, 2005
Revised May 3, 2005
Accepted June 7, 2005
Published online 11 July 2005)